LASEC: Instant Fabrication of Stretchable Circuits Using a Laser Cutter

Daniel Groeger
Saarland University
Saarland Informatics Campus
Saarbrücken, Germany
groeger@cs.uni-saarland.de

Jürgen Steimle
Saarland University
Saarland Informatics Campus
Saarbrücken, Germany
steimle@cs.uni-saarland.de

ABSTRACT

This paper introduces *LASEC*, the first technique for instant do-it-yourself fabrication of circuits with custom stretchability on a conventional laser cutter and in a single pass. The approach is based on integrated cutting and ablation of a two-layer material using parametric design patterns. These patterns enable the designer to customize the desired stretchability of the circuit, to combine stretchable with non-stretchable areas, or to integrate areas of different stretchability. For adding circuits on such stretchable cut patterns, we contribute routing strategies and a real-time routing algorithm. An interactive design tool assists designers by automatically generating patterns and circuits from a high-level specification of the desired interface. The approach is compatible with off-the-shelf materials and can realize transparent interfaces. Several application examples demonstrate the versatility of the novel technique for applications in wearable computing, interactive textiles, and stretchable input devices.

CCS CONCEPTS

• **Human-centered computing** → **Interactive systems and tools**.

KEYWORDS

Fabrication, stretchable circuits, rapid prototyping, laser cutting, laser ablation.

ACM Reference Format:
Daniel Groeger and Jürgen Steimle. 2019. LASEC: Instant Fabrication of Stretchable Circuits Using a Laser Cutter. In *CHI Conference on Human Factors in Computing Systems Proceedings (CHI 2019), May 4–9, 2019, Glasgow, Scotland UK*. ACM, New York, NY, USA, 14 pages. https://doi.org/10.1145/3290605.3300929

CHI 2019, May 4–9, 2019, Glasgow, Scotland UK

ACM ISBN 978-1-4503-5970-2/19/05.
https://doi.org/10.1145/3290605.3300929

1 INTRODUCTION

Stretchable interfaces are receiving growing attention. They allow designers to integrate interfaces in materials with elastic properties, such as textiles [32, 42] or human skin [44], and enable novel physical interactions [38].

However, creating functional prototypes to explore interaction with stretchable interfaces remains difficult. Prior work has relied on fabrication processes such as casting and sandwiching silicone layers with embedded conductors [26, 44, 46] or stitching conductive yarn in textiles [32, 42]. While these processes enable versatile circuit capabilities, they are time-consuming and rather complex. Moreover, existing techniques do not support the designer in easily defining the desired stretchability of a circuit, or including areas of different stretchability. These aspects are essential for many

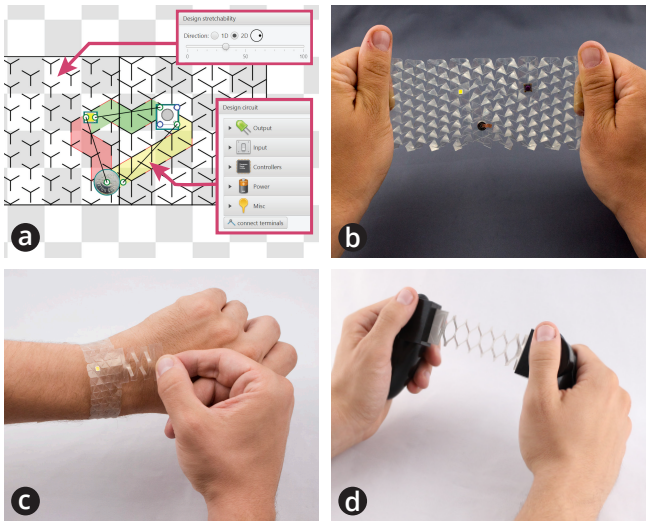

Figure 1: The LASEC technique uses a commodity laser cutter to fabricate stretchable circuits of custom stretchability, custom shape and with desired circuitry within minutes. (a) A design tool auto-generates cut-and-ablation patterns from a high-level specification of the circuit. (b) The resulting stretchable circuits can include electronic components, (c) can be transparent, and (c-d) support multiple areas of linear or omnidirectional stretchability.

interactive applications in HCI, which may require stretchable regions for buttons to push, rigid islands for mounting conventional electronic objects such as LEDs, or areas on wearable interfaces customized for the stretchability required on specific body locations.

In this paper, we present *LASEC*: Laser-fabricated Stretchable Circuits, the first instant technique for fabricating stretchable interfaces with custom circuitry and custom stretchability. Inspired by work in material science [4, 11, 40], it builds on parametric patterns of thin slits laser cut into a flexible compound material made of a non-conductive and a conductive layer. The pattern allows the surface to stretch at defined areas, in defined directions and up to a desired extent. In the same step, a custom electrical circuit is fabricated by using the laser at a lower intensity to ablate the conductive layer at specific locations.

LASEC delivers *instant* results, as it implements a one-step laser ablation and cutting process to create both single-layer circuitry and desired stretchable behavior of the interface in a single pass. This process overcomes the inherent limitations of multi-step approaches, which not only consume more time, but also partially rely on manual fabrication requiring expertise to achieve high-quality results. Fig. 1 illustrates several examples with stretchable circuits fabricated fully automatically in less than 5 minutes, a considerable improvement over fabrication times of state-of-the-art related work that reported one hour or multiple hours [26].

Furthermore, the approach is *accessible* to a broad audience, as it relies on a conventional laser cutter available in many labs, schools, and maker spaces. Lastly, the technique is *versatile*, since it is compatible with many materials of different properties, supporting custom circuitry and custom stretchability. This approach is thus suitable for a wide range of prototyping applications.

To realize LASEC, we contribute an approach for fabricating interfaces with one or multiple areas of customized stretchability, based on parametric cut patterns. The approach is the first to support user-defined areas with defined stretchability in one or multiple directions, seamless transitions between areas, and gradients of stretchability.

We further present the first approach to realize circuits on such stretchable structures produced by cut patterns. The major challenge is routing on these structures despite the bottlenecks created by the large number of cuts. We propose routing strategies for these structures and contribute a graph-based approach to enable real-time routing, which is crucial for instant feedback during the design step.

To assist designers in creating a custom stretchable circuit, we contribute a computational design tool. With a simple modeling application, it allows defining custom stretchable areas and the desired placement of electronic components at a high level of abstraction. The tool then automatically generates the cut-and-ablation patterns required to fabricate the custom design on the laser cutter.

We present four compatible materials, including low-cost DIY and off-the-shelf materials and materials for transparent stretchable circuits. We provide material recommendations for different use cases and a tool for automatic calibration of laser settings to enable easy replication of the approach. Results from a controlled technical evaluation validate that LASEC circuits enable more than 100% stretch in one dimension and up to 30% in two dimensions. They are mechanically and electrically durable for at least 1000 cycles of stretching. Three application examples show that LASEC enables rapid fabrication of stretchable circuits for a variety of prototyping applications, including wearables, smart textiles, and 3D-printed stretchable input devices.

2 RELATED WORK

Our contribution builds on prior work on laser fabrication, printed and stretchable electronics, and design tools.

Rapid fabrication using laser cutters

While laser cutters are commonly used for rapidly fabricating 2D shapes, recent research has investigated fabrication of 2.5D and 3D structures [3, 25, 39, 48]. These approaches combine regular cutting of standard materials [25, 39, 48] with different laser settings to achieve effects such as bending [25] or welding multiple layers [39]. FoldEm [3] uses a special multi-layer compound to fabricate foldable objects with joints of varying stiffness. Somewhat similar to our approach, this is achieved by ablating layers of different depth. Calibration of laser settings is done manually using smoke dye that was mixed into the compound material.

Laser machining is widely used for fabrication of soft robots and soft electronic devices (e.g., [24, 26, 44]). Elastic membranes, often silicone, are cut to the desired shapes and sandwiched manually. Laser cutters are also commonly used for do-it-yourself fabrication of rigid Printed Circuit Boards (PCBs), which involves several manual etching steps. Laser cutting and ablation are also employed in industrial manufacturing, e.g. to ablate a circuit design and subsequently cut the sample from a larger material sheet [14]. This is achieved with specialized laser devices that contain multiple laser sources of different wavelength optimized for a specific compound material [14].

Extending beyond this prior work, our approach is the first to create stretchable circuits using ablation and parametric cut patterns. It works with standard off-the-shelf material and standard laser cutters. We further provide a procedure that calibrates the correct laser settings automatically.

Fabricating custom deformable circuits for prototyping

Custom deformable circuits for prototyping are typically fabricated using printing techniques, e.g. inkjet printing [2, 15, 17, 34] and screen-printing [29], or embroidery [12, 33].

Research in this area has followed two major goals, as illustrated in Fig. 2: approaches that enable easy and rapid prototyping and novel techniques to extend the capabilities of do-it-yourself circuits towards those of professionally manufactured PCBs.

The instant inkjet circuit approach by Kawahara et al. [17] has demonstrated the key importance of rapid and accessible fabrication techniques for enabling and stimulating research in a range of application domains [6, 9, 15, 17, 27, 28, 34, 41]. PrintEm [2] contributes an alternative approach that requires a special material sandwich but uses regular ink instead of special conductive ink to increase accessibility.

Towards extended circuit capabilities, approaches based on screen-printing [29] and automated embroidery [12] have enabled the fabrication of multi-layer circuits, while screen-printing further added the ability to print displays [18, 21, 29, 30, 45] and actuators [29, 47] in addition to fabricating sensors. This, however, comes at a cost of more time-consuming processes, as well as required manual fabrication steps.

With a growing interest in stretchable interfaces, novel solutions are required to enable custom stretchable circuits. While initial work in this area has demonstrated how to realize stretchable sensors [32, 42, 44, 46, 49] and displays [46], recent research has demonstrated a considerably advanced fabrication technique that enables multi-layer stretchable devices including off-the-shelf components [26]. The approach combines silicone casting with laser patterning. While such approaches have an advantage in offering advanced circuit capabilities, e.g., to produce fully integrated devices, fabricating a prototype with these techniques typically takes multiple hours and requires expertise in silicone casting, manual sandwiching, or sewing.

In contrast, LASEC contributes a novel approach addressing two under-explored areas: It is the first rapid and accessible technique for prototyping stretchable circuits within minutes and without expertise in manual fabrication. It enables design and fabrication of custom stretchability in addition to custom circuitry, allowing the designer to computationally define multiple areas of custom stretchability.

Stretchability through cut patterns

Making flexible materials stretchable through cut patterns, often referred to as *Kirigami*, has been explored in material science and product design [4, 8, 10, 11, 20, 22, 40, 43]. The main principle is to cut a sheet so that the material deforms, e.g. buckles out-of-plane, at the cut locations when the sheet

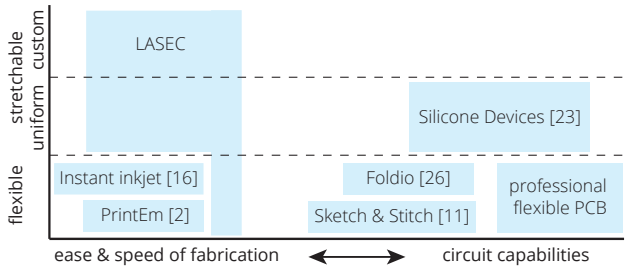

Figure 2: Related work on custom circuit fabrication techniques for prototyping.

undergoes tensile strain. We draw inspiration from these detailed studies on the mechanical behavior of different patterns in isolation and contribute the first work to support custom areas of different stretchability and seamless transitions in-between.

Pioneering work in material science has started to investigate the use of cut patterns for electronic components, typically at a micro-scale, for applications including supercapacitors for energy storage [11], stretchable graphene and metallic electrodes [1, 40], or stretchable nanocomposites as plasma electrodes [4]. Zhao et al. [51] have further proposed to 3D print silver wires on top of Kirigami-patterned PDMS. In contrast, our work is the first to present patterns designed for integrated circuits, i.e. routing paths through the stretch pattern using selective ablation.

Design tools for fabrication

Design tools for computational fabrication have been proposed to ease the complexity of manually designing functional objects. A variety of domains have been addressed by prior work, including laser cut mechanisms [5], 3D shapes made from sheet material [3, 19], or custom interactive objects and surfaces [27, 29, 34–36]. Our concept was inspired by the approach presented by Konakovic et al. [19], which generates a custom cut pattern that allows a sheet to wrap around a desired 3D geometry. In contrast, our approach and design tool address the unique challenges of stretchable circuits by automatically generating a cut pattern with areas of desired 1D or 2D stretchability and routing traces on the cut pattern.

3 INSTANT STRETCHABLE CIRCUITS WITH LASEC

We present a novel fabrication technique that allows designers, makers, and HCI researchers to fabricate stretchable circuits rapidly and with common lab tooling. Both stretchable behavior and electrical circuitry can be custom-designed. Figure 1 depicts several circuits that were fabricated using this technique. This section presents the basic principle and gives an overview of the design tool and fabrication process.

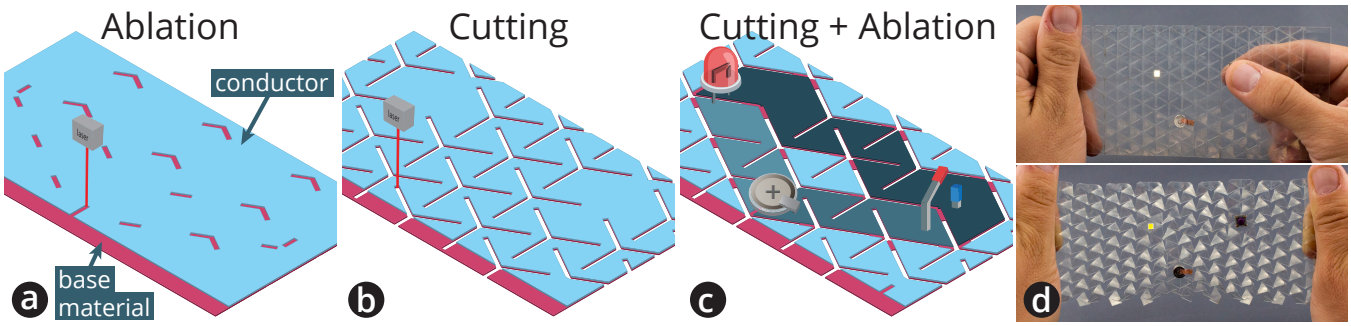

Figure 3: The LASEC principle combines ablation of the conductive top layer (a) with cutting of both material layers for stretchability (b) to create stretchable circuits (c). This example shows 3 created traces (c, highlighted) to connect an LED with a button and battery on a stretchable circuit (d).

Main Principle: Integrated Cutting and Ablation

The LASEC fabrication process works with a deformable two-layer compound material: a non-conductive base material is covered with a continuous conductive layer. This material by itself does not have to be stretchable. The key idea underlying the fabrication process is to combine two steps of subtractive fabrication that are both executed with a standard laser cutter in very little time (see Fig. 3): The deformable material is made stretchable by *cutting* slits into both layers using specific parametric patterns (Fig. 3b). These slits allow the surface to stretch when tensile force is applied (Fig. 3d). By adapting parameters of the pattern, the degree and direction of stretchability can be controlled. At the same time, traces of a custom stretchable circuit are created by selective *ablation* of the upper layer (Fig. 3a). During ablation, the laser operates at a lower power level to selectively vaporize patterns on the conductive top layer, while keeping the underlying base layer intact. By combining cutting and ablation (Fig. 3c) a stretchable circuit is created (Fig. 3d).

The principle is compatible with all common laser cutters. In fact, the approach could also work with other subtractive devices, e.g. milling machines. We use an Epilog Zing CO2 laser cutter, a common model available in many labs and maker spaces.

Any material compound can be used that is deformable, offers sufficient conductivity, and is compatible with laser cutting. Examples include commercially available ITO-coated (Indium Tin Oxide) sheets or standard plastic films coated with conductive ink or paint.

Overview of the Design and Fabrication Process

1. Digital design with design tool. The process starts with the digital design, which is the most crucial step. Creating a manual design for cutting and ablation that defines a desired stretchable behavior and electrical circuitry would be complex and time-consuming. It would also require the designer to have extensive knowledge of the mechanical and electrical properties of the material.

We contribute a design tool to make the technique accessible to a wide audience. It is depicted in Fig. 4. The tool allows the designer to easily specify the functional behavior at a high level. Using direct manipulation, the user specifies:

- the location, size, and shape of one or multiple stretchable areas, by drawing circles, rectangles, or 2D polygons
- the degree of stretchability of each area, by dragging a linear slider
- the direction of stretchability of each area: angle of linear stretchability or stretchable in both dimensions
- the electrical circuit, by placing components from a library[1] via drag-and-drop and specifying which terminals shall be connected by traces.

Based on this input specification, the tool automatically generates a custom-designed cut and ablation pattern, which is used as input for the laser cutter. Internally, the tool automatically maps the stretchability settings to the multiple low-level parameters of the cut pattern that together define the stretchable properties of the respective area. The tool then uses our novel routing approach, presented below, to compute the routing paths and to generate the required ablation pattern in real-time.

The design tool employs the designer-in-the-loop approach: The generated design is instantly visualized. Also while the user is dragging the stretchability slider, the generated cut pattern and circuitry is continuously updated. This allows the user to directly inspect the generated result.

2. Material selection. Next, the user chooses a compatible material compound to fabricate the stretchable circuit. We provide four material choices and recommendations on what materials to choose. A summary is provided in Table 1.

[1]The tool uses the Fritzing part format, with an open source library of more than 1500 components.

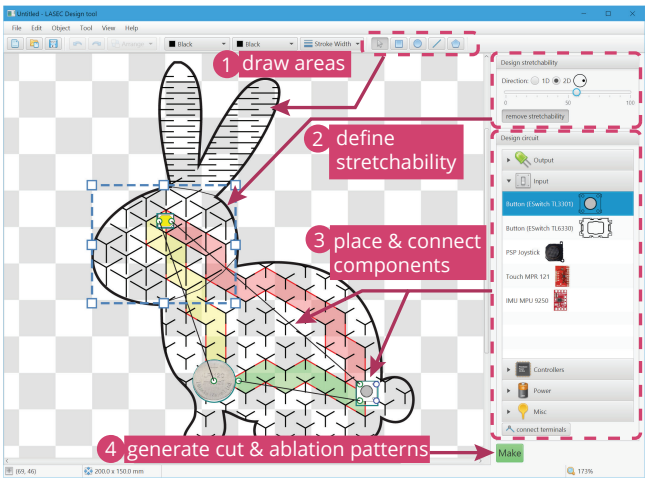

Figure 4: The LASEC design tool allows drawing areas and individually defining the stretchability and stretch direction of each area. Circuits can be defined by placing components from a library and connecting the required terminals. The tool immediately generates and visualizes the pattern parameterization and routing. To fabricate a design, it automatically generates the cut & ablation pattern.

The most accessible and easiest to use material option is *ITO-coated PET sheets*. ITO forms a fully transparent conductive layer of relatively high conductivity (60Ω/□). The compound material is available off-the-shelf (Sigma Aldrich 639303) and widely used in industry and DIY projects. However, the material has a comparably high cost (~$15/A4 sheet) and is less mechanically robust than our other options.

A cheaper and more versatile approach is to DIY coat a base material with a conductive layer, using a spray, brush or squeegee. A wide choice of conductive paint and inks is available. If high conductivity is a key requirement, we recommend commercially available *silver-nanoparticle (Ag) ink* (Gwent C2131014D3). With a low sheet resistance of 0.1Ω/□ it is suitable for high-fidelity circuits, e.g. including I2C, serial communication, or PWM. The most robust circuits can be fabricated using *PEDOT:PSS*, a conductive polymer that is intrinsically stretchable (Gwent C2100629D1), which however has a higher sheet resistance of 500 – 700Ω/□. Silver and PEDOT:PSS can be coated with a simple squeegee, a mayer rod, or a blade coater and cured at 80°*C* for 5 and 3 minutes respectively. *Carbon paint* (MG Chemicals 838AR, 1*k*Ω/□) can be easily applied by brushing, rolling, or spraying and does not need any post-processing. Despite higher sheet resistances, ITO, PEDOT:PSS, and carbon are still suitable for prototyping circuits, as has been demonstrated, e.g., for touch sensing [45, 46, 50] and EL-displays [29, 30, 46]. Carbon and PEDOT:PSS are the cheapest options (~$3/A4), with silver being slightly more expensive (~$4/A4).

Compound material	*Ease of use*	*Conductivity*	*Robustness*
ITO	●●●	●●○	●○○
Ag	●○○	●●●	●●○
PEDOT:PSS	●○○	●○○	●●●
Carbon	●●○	●○○	●●○

Table 1: Overview of compatible materials.

These coatings can be applied to a large variety of readily available prototyping materials. We recommend using laminating pouches and inkjet PET film, which are inexpensive ($0.05 and $1/A4) and result in elastic behavior with stretchability over 100% in one and up to 30% in two dimensions (see Evaluation section below).

For precise ablation of a given material on a laser cutter, the laser settings (i.e., power and speed) have to be calibrated once per material. This can be done manually by cutting traces on a material sample with increasing power until conductivity is lost. To ease this task for novice users and enable quicker exploration of additional various materials, we provide an automated calibration tool. It uses a simple breadboard-based resistance measuring device (microcontroller, Bluetooth module, and clips to connect to the material sample) that can be connected to a material sample and placed inside the laser cutter. A PC software rapidly determines cutting and ablation parameters for a given compound material. Schematics, controller firmware, and calibration software will be made available as open source for easy replication[2].

3. Laser cutting and ablation. The user places the material in the laser cutter and clicks on "Make" in the design tool. The tool generates a vector graphics file (SVG) color coded to represent laser settings, i.e. power and speed. The file is sent to the laser cutter, which fabricates the stretchable circuit fully automatically within a few minutes. The wristband and elbow patch in Fig. 5 were fabricated in 2 and 6 minutes respectively.

4. Connecting components. To finalize the device, the user connects wires and electronic components to the circuit, e.g., using conductive adhesives[3]. Placing components on "islands" in between cuts that undergo minimal deformation, as opposed to connections, improves adhesion.

To attach larger components, e.g. a microcontroller or a battery, the circuit can include "rigid" islands, a common practice in stretchable circuits, that can be easily designed and fabricated with LASEC as non-stretchable areas.

[2]https://hci.cs.uni-saarland.de/research/lasec

[3]We used 3M™ Z-Axis Conductive Tape 9703 and copper tape

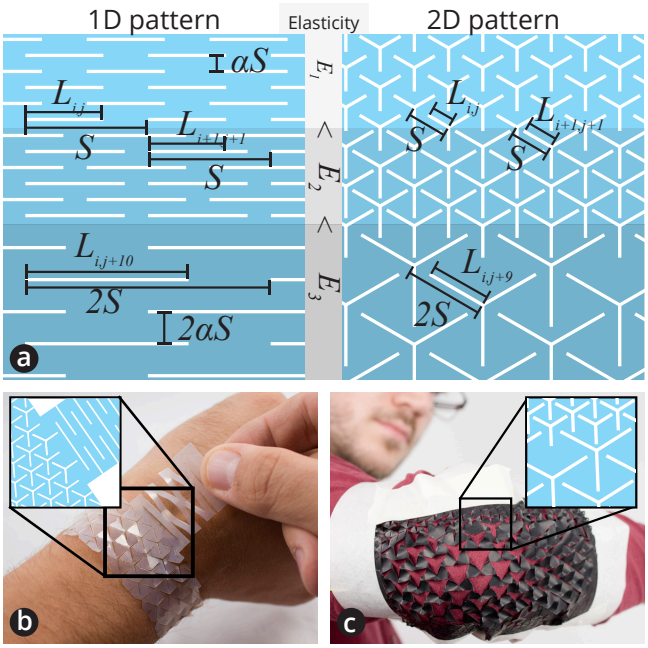

Figure 5: Interfaces can have multiple regions of different 1D stretch and 2D stretch behavior (a). To increase stretchability the cut ratio (L/S) is increased (from E_1 to E_2). To keep a minimal gap size ($S - L_{E_2}$), the cut ratio at E_2 cannot be increased further. To increase the stretchability beyond this limit, a scale transition is used (S is doubled). The bottom region E_3 is more stretchable than E_2, while its cut ratio is lower ($L_{E_3}/2S < L_{E_2}/S$) and the gap size wider ($2S - L_{E_3} > S - L_{E_2}$). These patterns allow interaction designers to define the direction of stretch (b) and to adapt the stretchability of different regions, e.g. to match stretch across joints (c).

4 PARAMETRIC CUT PATTERNS FOR CUSTOM STRETCHABILITY

This section presents parametric cut patterns that turn a deformable sheet into a stretchable surface. The key novelty is to allow designers to freely define custom areas of different stretchability and to support seamless transitions across areas. The patterns are chosen to be compatible with routing of circuits and auto-generated by the LASEC design tool.

Cut Patterns for Custom 1D and 2D Elastic Behavior

As an initial step, we identified parametric patterns suitable to be used for circuits. Two key requirements need to be met: First, to support routing and placement of components, the pattern should leave as much material connected as possible. This requires narrow cuts, while cutting holes or empty spaces should be avoided. This requirement excludes patterns based on auxetic beam-like or linkage-based structures, which have considerable empty space between beams [7, 16, 31, 37]. Second, the pattern must ensure that there is sufficient connected space in-between cuts for routing conductive traces. This contrasts with the common modeling of parametric cut patterns that treats connections between elements of the pattern as point connections without surface area [19].

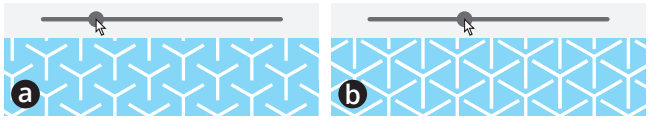

Figure 6: The tool allows adaptation of the stretchability of a region using a linear slider: e.g. from lower (a) to higher (b) stretchability.

1D Pattern: We base our parametric design on a pattern of parallel cuts, used in [4, 10, 11, 43], for its property allowing stretch in only one defined direction. Using this 1D pattern enables the designer to specify in which direction stretchability is desired. The pattern is shown in Fig. 5a. It offers considerable connected space for routing of circuitry, does not contain holes, and has been shown to support stretch up to 2000% in [10]. Two parameters influence the stretchability: L and S. Decreasing S or increasing L increases the stretchability, which scales with $\frac{(2L-S)^3}{S}$, as derived in [4] based on beam theory. A third parameter (α) is kept constant for alignment.

2D Pattern: To add the option of stretching in two dimensions, we use a second pattern. This pattern is based on Y-shaped cuts (as used in [40]). In contrast to the parallel alignment of the 1D pattern, cuts in the 2D pattern are oriented at 120 degree angles. Therefore, stress in multiple directions can be distributed across cuts, enabling adjacent regions with stretch in perpendicular directions. Hence, circuits can stretch over doubly-curved geometries.

The pattern has two parameters that affect the stretchability: L and S, see Fig. 5a. Increasing L or decreasing S increases the stretchability. Increasing both L and S while keeping L/S constant, i.e. scaling the entire pattern, also increases the stretchability. For a similar pattern, prior work has reported a logarithmic reduction in spring constant with a linear increase in L/S ratio [40]. In contrast to [40], we do not vary a third parameter w, the width of each cut, as this would introduce holes. Instead we keep the width of cuts at the minimum of the laser cutter (<0.3mm).

To support designers in directly and more intuitively defining the desired behavior, our design tool abstracts from these multiple low-level parameters. When the designer sets a desired stretchability using the linear slider, the tool automatically parameterizes the pattern accordingly (Fig. 6). We map the slider's value to a relative change in stretchability by adapting the L/S ratio of the pattern.

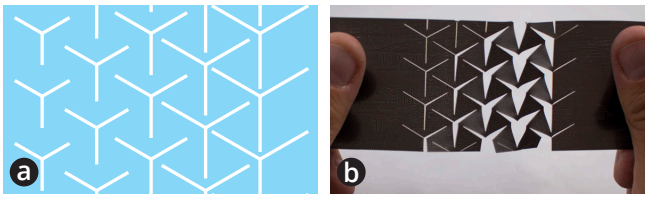

Figure 7: Using a gradient pattern from low to high stretchability (a) results in interfaces that stretch progressively from high to low with increasing force (b).

Multiple Areas of Different Elasticity

If the design contains two adjacent areas of different stretchability, alignment issues arise, as both cut patterns locally interact at the boundary in unforeseen ways. This results in inconsistent stretchable behavior and may create intersecting cuts that lead to holes in the material. We contribute a solution to create seamless transitions between adjacent areas. This also allows us to support stretchability gradients, where the stretchability continuously changes across an area.

Our approach keeps the grid for aligning the individual cut elements constant across areas of different stretchability. We call this the global *scale* of the pattern, i.e. the parameter S in the 1D and 2D patterns. As default we found $15mm$ and $5mm$ for 1D and 2D respectively to be a good compromise between little out-of-plane buckling and large stretchability. The stretchability of each area is then controlled by varying the size of the individual cut element. We call this the local *cut ratio*, i.e. L/S.

However, keeping the global scale fixed has its limitations. On the one hand, it may become necessary to use a larger scale, as it allows for a larger stretchability. This is easy to see: using a constant global scale, the stretchability of the pattern is increased by increasing the size of the cut elements. At one point, the element is as large as the grid size, preventing any further increase in size. On the other hand, it is also not desirable to always use a very large global scale, as this would result in larger out-of-plane buckling.

Our approach is to keep the scale of the pattern constant and as small as possible. Only if the desired stretchability exceeds the maximum stretchability supported by this scale is the scale increased by a factor of two. By only using multiples of the initial scale, the elements stay in a grid of even spacing for alignment (see Fig. 5a). The parameters of the local cut ratio (L/S) are adapted such that the desired stretchability is met. This results in overall larger cut elements but more space in-between cuts. This approach works with both cut patterns. Fig. 5c shows examples generated by our design tool that contain two directly adjacent areas of low and high stretchability and Fig. 7 a surface with a continuous stretchability gradient.

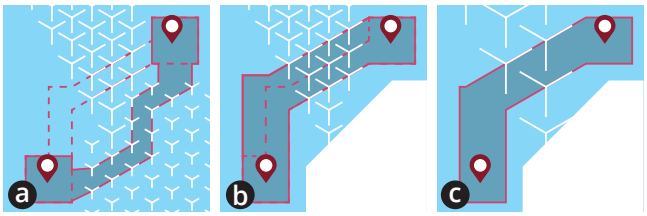

Figure 8: Three routing strategies allow coping with narrow bottlenecks to reduce a trace's resistance and increase its robustness by: (a) prioritizing areas of lower stretchability with wider bottlenecks (solid outline) over areas of higher stretchability (dashed outline), (b) routing via multiple adjacent paths through the pattern, or (c) adapting the cut pattern to increase the bottlenecks' width (compared to dashed outline in (a).

Adjacent areas of stretchability in different directions are enabled by the 2D pattern, as illustrated in Fig. 5b. In the example, the 2D pattern along the wrist enables stretching perpendicular to the 1D pattern, even in the top region where the patterns are connected. A 1D pattern would be constrained by the non-stretchable edge at the connection. Similarly, a 2D pattern enables stretchable regions enclosed within a non-stretchable region, e.g. for a stretchable push button. To combine a 1D and 2D pattern, a minimal space with no cuts is required to avoid alignment issues. In our implementation, this space is a strip as wide as the minimum trace width used for routing.

5 CIRCUIT ROUTING ON CUT PATTERNS

After generating the custom cut pattern for an interface of desired stretchability, the circuit is added by realizing conductive traces. Contrary to common conductive surfaces and printed circuit boards, the stretchable pattern contains a large number of cuts. These create serious bottlenecks for routing, which poses new challenges that were not addressed in prior work. We address them by proposing three general strategies for routing circuits on cut patterns and by contributing a novel routing algorithm that enables instant feedback while the designer is exploring design options (designer-in-the-loop approach).

Routing Strategies for Cut Patterns

We propose three general strategies for routing circuits on a stretchable cut pattern. These ensure that conductive traces of acceptable resistance can be routed between desired terminal points despite the bottlenecks created by the cut pattern. The strategies are implemented in our design tool:

Prioritize less stretchable areas. The first and simplest strategy is to prioritize areas with less stretchability. Those have wider bottlenecks than areas of higher stretchability (see

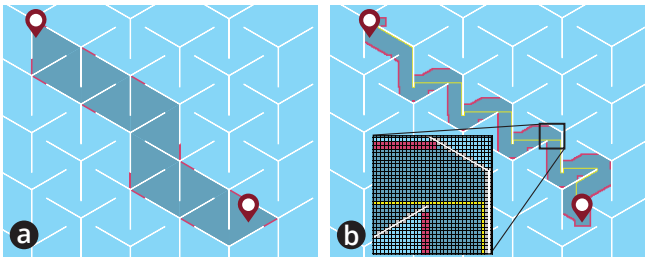

Figure 9: Comparison of routing result: our graph-based approach (a) requires a few nodes while maze routing requires a high resolution grid with many cells to model cuts as obstacles in sufficient detail (b).

Fig. 8a). Wider bottlenecks allow for wider traces, hence reducing the resistance. For example, Fig. 8aillustrates the shortest path through a region of lower stretchability has 82% wider bottlenecks than the 14% longer path through a region of higher stretchability (dashed outline); this reduces the resistance by 37%. It further enhances the mechanical robustness by virtue of less strain expected along the path. Areas with higher stretchability allow for larger stretch and thus may experience higher strain.

Our tool applies this strategy first, during initial routing of all traces. For each trace, the stretchability along its path in addition to its length is considered to find an optimal path. To this end, our tool uses the width of the bottlenecks of each area as weights in our graph representation for routing discussed below. This allows the tool to route traces along paths with less stretchability and wider bottlenecks for higher durability and lower resistance than shorter alternative paths.

Multipath routing. This strategy increases the conductivity of a connection across the cut pattern by using multiple parallel paths (see Fig. 8b). Fig. 8b illustrates the resistance between the two indicated points is approximately divided by two by using two parallel paths.

Our tool applies this strategy iteratively for all routed traces. For every trace, the tool checks for each bottleneck along the path to determine whether the trace can be widened by adding a parallel path through adjacent bottlenecks. For a single trace through a stretchable area, the tool widens the trace to the maximum extent. For multiple traces, the tool iteratively grows each trace in turn to find a common boundary between two adjacent traces.

Adapting the cut pattern. This strategy leverages the customizability of the cut pattern and adapts it to reduce or remove bottlenecks. The main limiting factor for routing of conductors at a bottleneck is the width of the remaining sheet's surface between two or more cuts (compare gap width $S - L$ in Fig. 5a). This width defines the effectively available area for routing.

This width can be enlarged without an effect on stretchability by increasing the overall scale of the pattern, as we have discussed in the previous section. Our tool applies this strategy if traces have a too high resistance despite applying the two previous strategies. Fig. 8c shows the bottlenecks to be 93% wider, reducing the resistance by 48%.

In some cases, the tool may not find a solution for routing all traces, e.g., in a case with many conductive traces, small bottlenecks, and little available space. The design tool then automatically determines if reducing the stretchability (and in turn reducing bottlenecks) would allow for solving this task. Internally, it incrementally reduces the stretchability of all areas and each time calculates possible routes until a solution is found or the stretchability cannot be further reduced. It then communicates to the designer that not all traces could be routed using the desired stretchability settings. The tool also indicates the reduced stretchability level for which it was able to generate a solution. The designer can then accept the less stretchable version or adapt the terminal placement for routing along a different path.

Real-time Routing on a Cut Pattern

To implement these routing strategies and to provide a fast approach to finding routes despite the many obstacles created by cuts, we propose a novel routing approach that runs in real time. This enables a designer-in-the-loop approach, where the designer can instantly see the effect of changes in stretchability on the generated routing.

In contrast, standard routing techniques, for instance Maze routing [23] as commonly used in prior work [29, 36], are not efficient for routing on cut patterns. For modeling the cut surface in sufficient detail, a very small grid size and hence a very large number of cells would be required. Even a small example[4] would require > 1 mio. grid cells and 126ms (on a 2.2GHz i7 CPU). Achieving a real-time update rate of at least 10Hz for circuits with ~10 traces would require a significantly shorter routing time of < 10ms per trace.

The key idea of our novel real-time approach is to leverage the repetitive structure of the pattern and model its geometry in a simplified graph structure, using pre-computed templates. Routes can then be calculated more efficiently on this graph using an existing graph-based routing algorithm.

Step 1: Offline generation of cell templates. The graph is constructed using offline pre-computed templates that model the routing-relevant properties of the pattern's basic elements, which we call cells. For a given parametric pattern, the cuts form the boundary of a repeating structure of tiled cells. The cell structures for our patterns are illustrated in Fig. 10a.

[4] 10x10cm sheet of 2D pattern ($L = 4.36mm$, $S = 5.45mm$) with three conductive traces; modeling this pattern requires a grid size of 0.1x0.1mm, as in Fig. 9b.

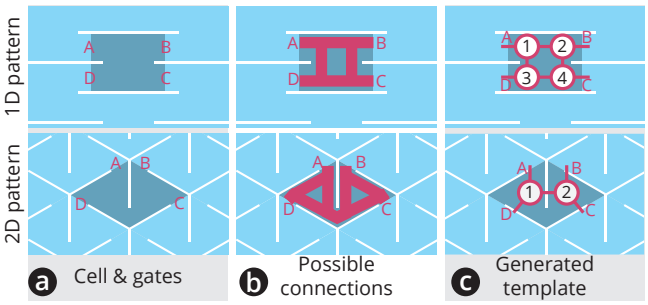

Figure 10: Pattern cells with gates labeled A-D (a), possible connections betweeen gates at given trace width (b), and the generated template with nodes and edges (c).

A cell consists of a *body* (its inner area) and several *gates* (openings where it connects to adjacent cells).

To automatically model the cell's routing-relevant properties with a minimum number of nodes during (offline) template creation, our algorithm computes how many connections can be routed across the gates and between gates inside the cell at a given minimal trace width (Fig. 10b). Note that this depends on the geometry of the gates and the space available in its body, which defines the cell's "bottlenecks". The algorithm creates a template that stores the number of nodes to be generated for the cell, the edges to be created between these nodes, and the "gate" edges to be created between these nodes and nodes of adjacent cells (Fig. 10c).

The template is created only once. Our tool stores templates in a database and performs a simple look-up for the correct template in the next step.

Step 2: Generating the routing graph. The entire graph is generated by adding one template for each cell of the pattern and then adding edges between nodes of adjacent cells connected through a gate.

For the example from above, the routing graph has 522 nodes and 737 edges (in contrast to >1 Mio. grid cells for Maze routing). Generating the graph takes $0.5ms$.

Step 3: Calculating routes. This compact graph representation then allows for efficient calculation of conductive routes using a graph-based routing algorithm. Our tool uses the A* algorithm [13] to route all traces of the circuit.

For the example from above, routing the three traces on the 10x10cm sheet takes $0.9ms$. This is about 140 times faster than the standard maze router and enables real-time feedback in the design tool.

Step 4: Generating ablation paths. When the user is satisfied with the routing and clicks "Make", our tool generates the ablation path. Since the entire sheet is one conductive layer, every routed trace needs to be isolated from the remaining surface through ablation. Since the entire surface is represented by our graph and conductive connections by edges, all locations are ablated that correspond to an edge connecting a routed path to the remaining graph. The final ablation pattern is stored color-coded in the SVG file sent to the cutter for fabrication.

6 VALIDATION

To validate the LASEC technique, we have empirically evaluated the main technical properties and furthermore demonstrated the practical feasibility by fabricating interfaces for 3 application cases.

Technical evaluation

In three technical experiments, we investigated material compatibility and electrical behavior and durability of stretchable circuits.

To this end, we subjected material samples to controlled stretch tests. We used a custom-built automatic extensometer that uses a linear actuator (Drive-Systems Europe DSZY1-Poti) controlled by a Teensy 3.5 microcontroller for stretching the sample by a defined displacement, once or repeatedly. The setup contains a precision multimeter (Fluke 8846) for four-point probe resistance measurement during stretching.

Material compatibility. For our initial pilot exploration of compatible materials, we collected and tested a broad selection of laser-compatible prototyping materials readily available online or in a hardware or office supply store. These include various types of plastic foils (plastic stretch wrap, vapor barrier foil, laminating pouches, overhead foil, inkjet PET film), acrylic sheets (Plexiglas) and acrylic films, paper, cardboard, wood veneer, leather, and cotton fabric.

While many materials could be coated, cut, and ablated, we identified two plastics (Fellowes laminating pouches and Mitsubishi inkjet PET film) to yield the most stretchable elastic deformation.

Next, we investigated the bounds of stretchability of the 1D and 2D patterns with different pattern parameters. We stretched four samples (5x10cm) of inkjet PET film in 5% increments to the point of rupture. The samples were cut with the 1D patterns of low stretchability (S=44, L=10, αS=3 mm) and high stretchability (S=44, L=40, αS=3 mm) as well as the 2D patterns of low (S=10.9, L=7.5 mm) and high (S=10.9, L=9.5 mm) stretchability.

Our results show a maximum stretch of 40% for the 1D low stretchability sample, while the 1D high stretchability pattern remained intact at 100% stretch, the limit of our stretch setup (20cm extension). In the 2D case, we found the low stretchability sample to rupture after 20% stretch and the high stretchability sample after 40% stretch.

	[kΩ]						[Ω]	
	Carbon		ITO		PEDOT		Ag	
Cycle	1D	2D	1D	2D	1D	2D	1D	2D
0	148.5	11.2	17.9	2.6	46.5	9.4	11.4	6.5
10	148.6	11.5	18.4	3.3	46.3	9.4	11.5	6.9
100	148.5	12.3	19.3	5.0	46.1	9.3	11.9	9.0
1000	148.7	14.6	20.6	11.7	46.2	9.5	12.7	17.6

Table 2: Baseline resistance after 0, 10, 100, and 1000 stretches.

Durability of stretchable circuits. In a dynamic durability test, we validated the endurance of the electrical functionality and mechanical integrity of LASEC circuits. We add to findings from prior work in material science that has used different materials and parameters [11, 40]. We subjected samples (5x10cm) made of four conductive materials (ITO, sprayed carbon, and silver and PEDOT:PSS applied with squeegee on PET film) and cut with both patterns (1D and 2D) to 1000 repeated stretching cycles. Based on the previous results, we selected the pattern parameters for high stretchability, which represent an upper bound and thus the most challenging conditions. We stretched the samples by 100% in the 1D and 30% in the 2D case (10% safety margin to point before rupture). We continuously measured the resistance.

Absolute measurements of baseline resistance after 0, 10, 100 and 1000 stretching cycles are given in Table 2. The results show that all materials with both patterns remain functional after 1000 stretching cycles.

PEDOT shows a very small change in baseline resistance for both patterns (~1%), indicating high durability. This compares favorably with the behavior of recent state-of-the-art DIY solutions for stretchable devices in HCI that use liquid metals in silicone casts.[5]

The other materials also achieve suitable durability, especially for prototyping purposes, where the range of < 100 stretches is most relevant. Compared to related work, even the largest baseline drift after 1000 cycles (ITO with 2D pattern: ~350% increase) is an order of magnitude lower than results reported on DIY stretchable displays using conductive polymer printed on silicone.[6] While PEDOT:PSS also compares favorably with results of deposited metal films [40], the other materials may benefit from the approach of [40]. It shows improved robustness for a horseshoe-style variant of the pattern, while offering, however, only minimal surface area to attach components.

This high endurance, despite brittle silver and ITO conductors, can be explained by the fact that common approaches physically elongate the material while stretched, while our cut patterns allow elastic deformation by bending material out-of-plane at the connection points between cells. This significantly reduces stress [40] on the conductive traces.

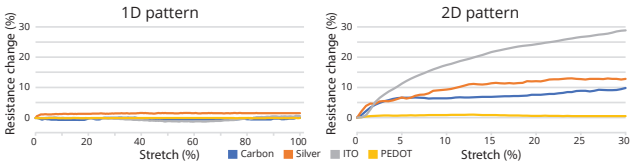

Figure 11: Relative change in resistance during stretch of 1D pattern (left) and 2D pattern (right).

Behavior during stretching. Fig. 11 depicts the effect of stretch on resistance during a stretching cycle, for the 1D and 2D pattern and all four conductive materials. For 1D stretch of 100%, the relative change of resistance remains below 2% for all materials. This is in line with results for other materials, which show a low change for stretch up to 300% [43] or even 2000% [10]. This change is below tolerances of common resistors (5%) and thus has no significant effect on the circuit. For 2D stretch of 30%, the relative resistance change remains within a typical range for stretchable circuits ($1 - 30\%$).[7]

This relatively small effect of stretch on resistance also holds true after the sample underwent repeated stretching and releasing cycles. After 1000 cycles, PEDOT:PSS and carbon show the same resistance increase of 1% and 10% respectively. Silver exhibits a change below 30% for the first 100 cycles and settles around 35% after ~200 cycles. ITO shows a larger (60%) increase during initial stretching, likely due to micro cracks forming, which decreases to ~30% after 10 cycles (as shown in Fig. 11) and settles at ~10% after 50 cycles. Based on these results, we recommend initializing ITO by stretching 10 times before using it with a 2D pattern. We further recommend PEDOT:PSS as the most robust material, as it is least affected by stretch, with a relative change of $< 1\%$ in all cases.

Example applications and use cases

We validated the suitability of LASEC for prototyping stretchable interfaces by implementing three applications for interactive accessories, physical input devices, and interactive clothing. The applications demonstrate LASEC's rapid fabrication speed, support of circuits with high frequency signals, and simple stretch sensing, alongside its capability of realizing circuits of custom stretchability.

Interactive transparent wristband. To demonstrate the fabrication of transparent stretchable interfaces and integrating areas of very differing stretch properties, we implemented

[5] [26] reported a resistance increase of 5.7% after 1000 cycles at 200% strain.
[6] 6450% after 10 stretching cycles at 50% strain [46]

[7] For comparison, [44] reported a 32.4% increase at 30% stretch; [26] reported a $\sim 60 - 250\%$ increase at $30 - 100\%$ stretch.

an interactive stretchable wristband using ITO, shown in Fig. 12b. It features an LED for output and allows the user to interact using two gestures: pulling on the band itself, which is enabled by a 2D stretchable area along the band, and pulling an additional orthogonal strap, which is inspired by a watch crown and realized with a 1D stretchable area (Fig. 1c). In our example application, the wristband is used as a countdown timer for running. Pulling the strap is mapped to the frequent action of starting/stopping the timer. Resetting the timer is performed by pulling the band.

The stretchable circuit on the wristband contains four traces: two for controlling the LED, one for sensing pulling on the band, and one for sensing pulling on the orthogonal strap (Fig. 12a).

The six endpoints are tethered to a Teensy 3.5 microcontroller, a voltage divider, and a battery. By measuring the resistance across both sensing traces, we can detect both gestures using a simple thresholding approach.

To explore the desired stretchability for both pulling interactions and to ensure a comfortable fit of the wristband, we quickly iterated over the design. Using LASEC, adapting the stretchability and fabricating the design for one iteration takes less than 2 minutes. We reached the final design after 4 iterations (Fig. 12a) and within 10 minutes.

3D-printed stretchable game controller. LASEC circuits allow rapid prototyping in many scenarios where custom stretchability is key. In this example, we are prototyping a custom 3D-printed stretchable game controller, shown in Fig. 12c and d. It features two 3D-printed handles, which are connected with a custom stretchable circuit on silver-coated PET. One inertial measurement unit (IMU) in each handle allows inferring their relative position, while one button allows triggering actions. The circuit also contains a commodity Teensy 3.2 microcontroller.

The 3D-printed handles themselves are passive and printed on a conventional 3D printer (Objet260 Connex3). All interactive functionality is added through a single stretchable circuit that was fabricated using LASEC. The circuit features two non-stretchable areas for holding the components inside each handle, and a stretchable center area that contains four traces for connecting the IMU in the left handle with the microcontroller in the right handle using I^2C.

Textile sensor patch for joint angle estimation. We implemented a smart textile patch, worn on the elbow, that contains an integrated stretch sensor for capturing the angle of the elbow joint (see Fig. 12e). This application demonstrates LASEC's support for custom-shaped designs, multiple seamlessly connected stretchable areas, and simple integrated stretch sensing. The stretchable interface features two concentric, elliptical areas that are stretchable in 2D: a less stretchable outer area, where the patch is attached, and

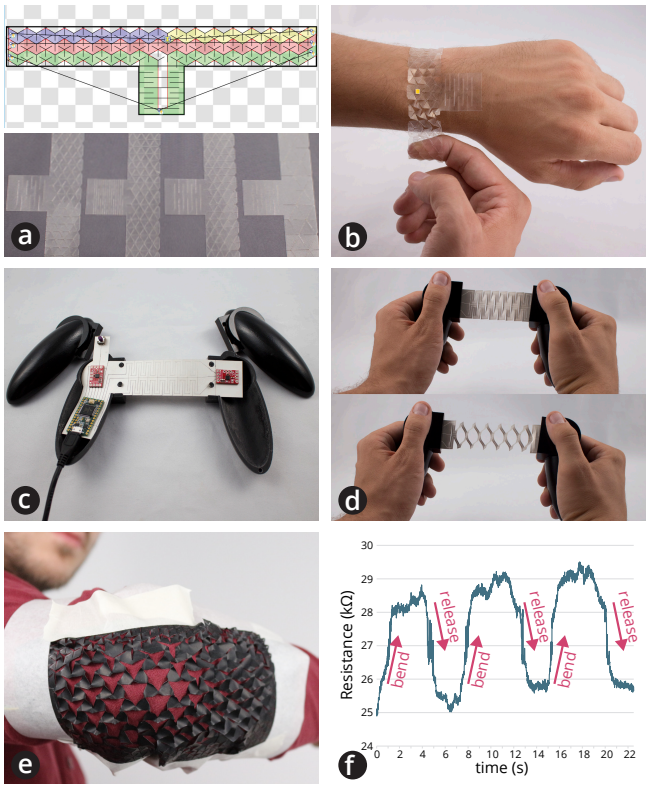

Figure 12: Example applications: wristband design with four fabricated prototypes (a) and a pull gesture being performed (b), game controller circuit (c) and prototype being stretched state (d), and textile sensor patch on bent elbow (e) and resistance reading for 3 bending cycles (f).

a more stretchable inner area that stretches when the joint is bent. A conductive trace was laid out on the stretchable surface such that it undergoes a large physical deformation when the inner area is stretched.

We chose carbon as a conductive material due to its suitable properties (robustness and consistent change in resistance) for stretch sensing. The stretchable circuit was laser-fabricated within 6 minutes. A small Teensy 3.5 microcontroller, voltage divider, and a battery were connected to the circuit. Using a conservative mapping, the continuous signal of resistance change, e.g. plotted in Fig. 12f, is mapped to one of four discrete bending states. We attached the finished patch onto the elbow region of a long-sleeve shirt. A user wearing the shirt can thus interact through arm gestures that are captured using the stretchable circuit.

7 LIMITATIONS

The benefits of the LASEC approach – a considerable speed-up of stretchable circuit fabrication and a customizable stretch behavior of the circuit – come with several limitations:

First, our approach is currently restricted to single-layer circuits to enable rapid and simple fabrication. In contrast, multi-layer approaches would require a manual multi-step process. This may introduce misalignment issues because a sheet needs to be removed from the laser cutter for a subsequent coating or a double-sided sheet needs to be manually flipped over. From our experiments, we can report anecdotally that VIAs for two-layer circuits can be realized using multiple subsequent coatings. After ablating the first conductive layer, a dielectric layer (GWENT D2180423D3) is coated on top. VIA locations are then ablated in the dielectic layer and finally a second conductive layer is coated and ablated to form the second circuit layer. In future work, we plan to investigate this extension to multi-layer circuits and address the resulting alignment problem, e.g., through visual markers or a detachable alignment frame on the cutting bed.

The supported complexity of single-layer circuits with LASEC depends on the width of ablation paths and material conductivity. With our laser we can ablate paths of $\sim mm$ width. Silver traces down to $\sim 0.3mm$ width yield a reasonable resistance ($3.3\frac{\Omega}{cm}$). This results in a minimum width of $\sim 0.4mm$ per trace and makes it possible to pass multiple traces through one connecting point of the 1D pattern (as illustrated in Fig. 5) or 2D pattern. As an example, we were able to route 20 wires through the pattern of the controller (Fig 12c), with a bottleneck width of $8mm$. A cell between two of such connectors could thus hold a 40-pin component with a minimum pitch of $\sim 0.4mm$.

The minimum size of a stretchable circuit is defined by the minimum width of the connecting elements required for mechanically stable connections. In our case, this is 1.6mm, resulting in a minimum pattern spacing of $S = 2.88$mm at a mimimum stretchability ($\frac{L}{S} = 0.6$). For our selected materials, we fabricated circuits as small as 7x7mm (3x3 cells). The maximum size of a stretchable interface is limited by the size of the laser cutter's bed. Various approaches have been investigated to extend beyond this general restriction of laser fabrication, such as side-ways sliding of the sample. These approaches are compatible with LASEC, provided they keep the sample at a constant distance from the laser.

Our design tool is based on parametric models that describe the stretchable behavior of the material. We opted against including a module for physical simulation because finite element modeling (FEM), which is required to simulate our 2D pattern, is too computationally intense to comply with the hard real-time constraint of our designer-in-the-loop modeling approach (>10Hz updates). Future work may investigate how to incorporate such a simulation, as it could provide helpful insights into stress concentration and material-dependent behavior.

During stretch, the fabricated circuits exhibit a unique deformation behavior due to the out-of-plane buckling for stress relief. In some cases, this may be undesirable. In these cases, LASEC can be a very helpful tool for rapid iterations in early prototyping, while a more time-consuming approach (e.g., based on silicon) may be used for the final high-fidelity product. Future work may be able to reduce the buckling by minimizing the patterns' scales, possibly down to the micro- or even nano-scale [40].

Laser ablation is used on flat materials, as the laser is focused on a specific distance. This excludes materials with a coarse surface structure as well as 3D-shaped objects. Future work could investigate automatic focusing of the laser or automatic positioning of 3D objects [25] to support fabrication of stretchable 3D objects with LASEC.

8 CONCLUSION

In this paper, we have contributed LASEC, the first instant technique for fabricating stretchable interfaces with custom circuitry and custom stretchability. LASEC combines laser cutting of parametric patterns for stretchability with ablation for custom circuits. A design tool allows the user to specify the stretchable and electrical properties of the circuit and auto-generates the files for laser cutting. We have introduced the technique and presented novel approaches that address the technical challenges to realize LASEC. These include generating cut patterns for multiple areas of customized stretchability and a novel approach to realize circuits on such cut patterns. Results from an empirical evaluation and from a range of application examples demonstrate the practical feasibility and versatility of the approach.

In future work, we want to explore more diverse materials with the goal to further increase the maximum stretchability of LASEC circuits. We also plan to replicate the LASEC approach on a milling machine or a fiber laser to explore the use of pure metallic conductors, which would further increase the conductivity. Future work should also investigate how to extend the LASEC approach to enable multi-layer circuits and to support 3D-shaped objects.

ACKNOWLEDGMENTS

This project received funding from the European Research Council (ERC) under the European Union's Horizon 2020 research and innovation program (grant agreement No 714797, StG Interactive Skin) and the Cluster of Excellence on Multimodal Computing and Interaction. We thank Sven Ehses for his help with the calibration tool, evaluation, and fabrication of application examples and Aditya Shekhar Nittala and Muhammad Hamid for their help with video editing.

REFERENCES

[1] D. A. Bahamon, Zenan Qi, Harold S. Park, Vitor M. Pereira, and David K. Campbell. 2016. Graphene kirigami as a platform for stretchable and tunable quantum dot arrays. *Phys. Rev. B* 93 (Jun 2016), 235408. Issue 23. https://doi.org/10.1103/PhysRevB.93.235408

[2] Varun Perumal C and Daniel Wigdor. 2015. Printem: Instant Printed Circuit Boards with Standard Office Printers & Inks. In *Proceedings of the 28th Annual ACM Symposium on User Interface Software & Technology (UIST '15)*. ACM, New York, NY, USA, 243–251. https://doi.org/10.1145/2807442.2807511

[3] Varun Perumal C and Daniel Wigdor. 2016. Foldem: Heterogeneous Object Fabrication via Selective Ablation of Multi-Material Sheets. In *Proceedings of the 2016 CHI Conference on Human Factors in Computing Systems (CHI '16)*. ACM, New York, NY, USA, 5765–5775. https://doi.org/10.1145/2858036.2858135

[4] Terry C Shyu, Pablo Damasceno, Paul M Dodd, Aaron Lamoureux, Lizhi Xu, Matthew Shlian, Max Shtein, Sharon C Glotzer, and Nicholas Kotov. 2015. A kirigami approach to engineering elasticity in nanocomposites through patterned defects. *Nature materials* 14 (06 2015).

[5] Stelian Coros, Bernhard Thomaszewski, Gioacchino Noris, Shinjiro Sueda, Moira Forberg, Robert W. Sumner, Wojciech Matusik, and Bernd Bickel. 2013. Computational Design of Mechanical Characters. *ACM Trans. Graph.* 32, 4, Article 83 (July 2013), 12 pages. https://doi.org/10.1145/2461912.2461953

[6] Nan-Wei Gong, Jürgen Steimle, Simon Olberding, Steve Hodges, Nicholas Edward Gillian, Yoshihiro Kawahara, and Joseph A. Paradiso. 2014. PrintSense: A Versatile Sensing Technique to Support Multimodal Flexible Surface Interaction. In *Proceedings of the SIGCHI Conference on Human Factors in Computing Systems (CHI '14)*. ACM, New York, NY, USA, 1407–1410. https://doi.org/10.1145/2556288.2557173

[7] Joseph N Grima, Ruben Gatt, Andrew Alderson, and KE Evans. 2005. On the potential of connected stars as auxetic systems. *Molecular Simulation* 31, 13 (2005), 925–935.

[8] Joseph N. Grima, Ruben Gatt, Brian Ellul, and Elaine Chetcuti. 2010. Auxetic behaviour in non-crystalline materials having star or triangular shaped perforations. *Journal of Non-Crystalline Solids* 356, 37 (2010), 1980 – 1987. https://doi.org/10.1016/j.jnoncrysol.2010.05.074 Joint Conferences on Advanced Materials: Functional and Nanonstructured Materials - FNMA'09; Intermolecular and Magnetic Interactions in Matter - IMIM'09.

[9] Daniel Groeger, Elena Chong Loo, and Jürgen Steimle. 2016. HotFlex: Post-print Customization of 3D Prints Using Embedded State Change. In *Proceedings of the 2016 CHI Conference on Human Factors in Computing Systems (CHI '16)*. ACM, New York, NY, USA, 420–432. https://doi.org/10.1145/2858036.2858191

[10] Ying-Shi Guan, Zhuolei Zhang, Yichao Tang, Jie Yin, and Shenqiang Ren. 2018. Kirigami-Inspired Nanoconfined Polymer Conducting Nanosheets with 2000% Stretchability. *Advanced Materials* 30, 20 (2018), 1706390. https://doi.org/10.1002/adma.201706390

[11] Hengyu Guo, Min-Hsin Yeh, Ying-Chih Lai, Yunlong Zi, Changsheng Wu, Zhen Wen, Chenguo Hu, and Zhong Lin Wang. 2016. All-in-One Shape-Adaptive Self-Charging Power Package for Wearable Electronics. *ACS Nano* 10, 11 (2016), 10580–10588. https://doi.org/10.1021/acsnano.6b06621 PMID: 27934070.

[12] Nur Al-huda Hamdan, Simon Voelker, and Jan Borchers. 2018. Sketch&Stitch: Interactive Embroidery for E-textiles. In *Proceedings of the 2018 CHI Conference on Human Factors in Computing Systems (CHI '18)*. ACM, New York, NY, USA, Article 82, 13 pages. https://doi.org/10.1145/3173574.3173656

[13] P. E. Hart, N. J. Nilsson, and B. Raphael. 1968. A Formal Basis for the Heuristic Determination of Minimum Cost Paths. *IEEE Transactions on Systems Science and Cybernetics* 4, 2 (July 1968), 100–107. https://doi.org/10.1109/TSSC.1968.300136

[14] Joe Hillman, Yefim Sukhman, and Chris Risser. 2015. Multiple Wavelength Laser Processing Technology for Flexible Manufacturing. *Lasers in Manufacturing Conference 2015* (2015).

[15] Steve Hodges, Nicolas Villar, Nicholas Chen, Tushar Chugh, Jie Qi, Diana Nowacka, and Yoshihiro Kawahara. 2014. Circuit Stickers: Peel-and-stick Construction of Interactive Electronic Prototypes. In *Proceedings of the 32Nd Annual ACM Conference on Human Factors in Computing Systems (CHI '14)*. ACM, New York, NY, USA, 1743–1746. https://doi.org/10.1145/2556288.2557150

[16] Alexandra Ion, Johannes Frohnhofen, Ludwig Wall, Robert Kovacs, Mirela Alistar, Jack Lindsay, Pedro Lopes, Hsiang-Ting Chen, and Patrick Baudisch. 2016. Metamaterial Mechanisms. In *Proceedings of the 29th Annual Symposium on User Interface Software and Technology (UIST '16)*. ACM, New York, NY, USA, 529–539. https://doi.org/10.1145/2984511.2984540

[17] Yoshihiro Kawahara, Steve Hodges, Benjamin S. Cook, Cheng Zhang, and Gregory D. Abowd. 2013. Instant Inkjet Circuits: Lab-based Inkjet Printing to Support Rapid Prototyping of UbiComp Devices. In *Proceedings of the 2013 ACM International Joint Conference on Pervasive and Ubiquitous Computing (UbiComp '13)*. ACM, New York, NY, USA, 363–372. https://doi.org/10.1145/2493432.2493486

[18] Konstantin Klamka and Raimund Dachselt. 2017. IllumiPaper: Illuminated Interactive Paper. In *Proceedings of the 2017 CHI Conference on Human Factors in Computing Systems (CHI '17)*. ACM, New York, NY, USA, 5605–5618. https://doi.org/10.1145/3025453.3025525

[19] Mina Konaković, Keenan Crane, Bailin Deng, Sofien Bouaziz, Daniel Piker, and Mark Pauly. 2016. Beyond Developable: Computational Design and Fabrication with Auxetic Materials. *ACM Trans. Graph.* 35, 4, Article 89 (July 2016), 11 pages. https://doi.org/10.1145/2897824.2925944

[20] Valentin Kunin, Shu Yang, Yigil Cho, Pierre Deymier, and David J. Srolovitz. 2016. Static and dynamic elastic properties of fractal-cut materials. *Extreme Mechanics Letters* 6 (2016), 103 – 114. https://doi.org/10.1016/j.eml.2015.12.003

[21] Stacey Kuznetsov, Piyum Fernando, Emily Ritter, Cassandra Barrett, Jennifer Weiler, and Marissa Rohr. 2018. Screenprinting and TEI: Supporting Engagement with STEAM Through DIY Fabrication of Smart Materials. In *Proceedings of the Twelfth International Conference on Tangible, Embedded, and Embodied Interaction (TEI '18)*. ACM, New York, NY, USA, 211–220. https://doi.org/10.1145/3173225.3173253

[22] Haresh Lalvani. 2011. Multi-directional and variably expanded sheet material surfaces.

[23] C. Y. Lee. 1961. An Algorithm for Path Connections and Its Applications. *IRE Transactions on Electronic Computers* EC-10, 3 (Sept 1961), 346–365. https://doi.org/10.1109/TEC.1961.5219222

[24] Tong Lu, Lauren Finkenauer, James Wissman, and Carmel Majidi. 2014. Rapid Prototyping for Soft-Matter Electronics. *Advanced Functional Materials* 24, 22 (2014), 3351–3356. https://doi.org/10.1002/adfm.201303732

[25] Stefanie Mueller, Bastian Kruck, and Patrick Baudisch. 2013. LaserOrigami: Laser-cutting 3D Objects. In *Proceedings of the SIGCHI Conference on Human Factors in Computing Systems (CHI '13)*. ACM, New York, NY, USA, 2585–2592. https://doi.org/10.1145/2470654.2481358

[26] Steven Nagels, Raf Ramakers, Kris Luyten, and Wim Deferme. 2018. Silicone Devices: A Scalable DIY Approach for Fabricating Self-Contained Multi-Layered Soft Circuits Using Microfluidics. In *Proceedings of the 2018 CHI Conference on Human Factors in Computing Systems (CHI '18)*. ACM, New York, NY, USA, Article 188, 13 pages. https://doi.org/10.1145/3173574.3173762

[27] Hyunjoo Oh, Tung D Ta, Ryo Suzuki, Mark D Gross, Yoshihiro Kawahara, and Lining Yao. 2018. PEP (3D Printed Electronic Papercrafts): An integrated approach for 3D sculpting paper-based electronic devices. In *Proceedings of the 2018 CHI Conference on Human Factors in Computing Systems (CHI '18)*. ACM, New York, NY, USA, to appear.

[28] Simon Olberding, Nan-Wei Gong, John Tiab, Joseph A. Paradiso, and Jürgen Steimle. 2013. A Cuttable Multi-touch Sensor. In *Proceedings of the 26th Annual ACM Symposium on User Interface Software and Technology (UIST '13)*. ACM, New York, NY, USA, 245–254. https://doi.org/10.1145/2501988.2502048

[29] Simon Olberding, Sergio Soto Ortega, Klaus Hildebrandt, and Jürgen Steimle. 2015. Foldio: Digital Fabrication of Interactive and Shape-Changing Objects With Foldable Printed Electronics. In *Proceedings of the 28th Annual ACM Symposium on User Interface Software & Technology (UIST '15)*. ACM, New York, NY, USA, 223–232. https://doi.org/10.1145/2807442.2807494

[30] Simon Olberding, Michael Wessely, and Jürgen Steimle. 2014. PrintScreen: Fabricating Highly Customizable Thin-film Touch-displays. In *Proceedings of the 27th Annual ACM Symposium on User Interface Software and Technology (UIST '14)*. ACM, New York, NY, USA, 281–290. https://doi.org/10.1145/2642918.2647413

[31] Jifei Ou, Zhao Ma, Jannik Peters, Sen Dai, Nikolaos Vlavianos, and Hiroshi Ishii. 2018. KinetiX - designing auxetic-inspired deformable material structures. *Computers & Graphics* (2018). https://doi.org/10.1016/j.cag.2018.06.003

[32] Patrick Parzer, Kathrin Probst, Teo Babic, Christian Rendl, Anita Vogl, Alex Olwal, and Michael Haller. 2016. FlexTiles: A Flexible, Stretchable, Formable, Pressure-Sensitive, Tactile Input Sensor. In *Proceedings of the 2016 CHI Conference Extended Abstracts on Human Factors in Computing Systems (CHI EA '16)*. ACM, New York, NY, USA, 3754–3757. https://doi.org/10.1145/2851581.2890253

[33] E. R. Post, M. Orth, P. R. Russo, and N. Gershenfeld. 2000. E-broidery: Design and Fabrication of Textile-based Computing. *IBM Syst. J.* 39, 3-4 (July 2000), 840–860. https://doi.org/10.1147/sj.393.0840

[34] Raf Ramakers, Kashyap Todi, and Kris Luyten. 2015. PaperPulse: An Integrated Approach for Embedding Electronics in Paper Designs. In *Proceedings of the 33rd Annual ACM Conference on Human Factors in Computing Systems (CHI '15)*. ACM, New York, NY, USA, 2457–2466. https://doi.org/10.1145/2702123.2702487

[35] Valkyrie Savage, Sean Follmer, Jingyi Li, and Björn Hartmann. 2015. Makers' Marks: Physical Markup for Designing and Fabricating Functional Objects. In *Proceedings of the 28th Annual ACM Symposium on User Interface Software & Technology (UIST '15)*. ACM, New York, NY, USA, 103–108. https://doi.org/10.1145/2807442.2807508

[36] Valkyrie Savage, Xiaohan Zhang, and Björn Hartmann. 2012. Midas: Fabricating Custom Capacitive Touch Sensors to Prototype Interactive Objects. In *Proceedings of the 25th Annual ACM Symposium on User Interface Software and Technology (UIST '12)*. ACM, New York, NY, USA, 579–588. https://doi.org/10.1145/2380116.2380189

[37] F Scarpa, P Panayiotou, and G Tomlinson. 2000. Numerical and experimental uniaxial loading on in-plane auxetic honeycombs. *The Journal of Strain Analysis for Engineering Design* 35, 5 (2000), 383–388. https://doi.org/10.1243/0309324001514152

[38] Giovanni Maria Troiano, Esben Warming Pedersen, and Kasper Hornbæk. 2015. Deformable Interfaces for Performing Music. In *Proceedings of the 33rd Annual ACM Conference on Human Factors in Computing Systems (CHI '15)*. ACM, New York, NY, USA, 377–386. https://doi.org/10.1145/2702123.2702492

[39] Udayan Umapathi, Hsiang-Ting Chen, Stefanie Mueller, Ludwig Wall, Anna Seufert, and Patrick Baudisch. 2015. LaserStacker: Fabricating 3D Objects by Laser Cutting and Welding. In *Proceedings of the 28th Annual ACM Symposium on User Interface Software & Technology (UIST '15)*. ACM, New York, NY, USA, 575–582. https://doi.org/10.1145/2807442.2807512

[40] Nicolas Vachicouras, Christina M. Tringides, Philippe B. Campiche, and Stéphanie P. Lacour. 2017. Engineering reversible elasticity in ductile and brittle thin films supported by a plastic foil. *Extreme Mechanics Letters* 15 (2017), 63–69. https://doi.org/10.1016/j.eml.2017.05.005

[41] Nirzaree Vadgama and Jürgen Steimle. 2017. Flexy: Shape-Customizable, Single-Layer, Inkjet Printable Patterns for 1D and 2D Flex Sensing. In *Proceedings of the Eleventh International Conference on Tangible, Embedded, and Embodied Interaction (TEI '17)*. ACM, New York, NY, USA, 153–162. https://doi.org/10.1145/3024969.3024989

[42] Anita Vogl, Patrick Parzer, Teo Babic, Joanne Leong, Alex Olwal, and Michael Haller. 2017. StretchEBand: Enabling Fabric-based Interactions Through Rapid Fabrication of Textile Stretch Sensors. In *Proceedings of the 2017 CHI Conference on Human Factors in Computing Systems (CHI '17)*. ACM, New York, NY, USA, 2617–2627. https://doi.org/10.1145/3025453.3025938

[43] Zhihui Wang, Ling Zhang, Shasha Duan, Hao Jiang, Jianhua Shen, and Chunzhong Li. 2017. Kirigami-patterned highly stretchable conductors from flexible carbon nanotube-embedded polymer films. *J. Mater. Chem. C* 5 (2017), 8714–8722. Issue 34. https://doi.org/10.1039/C7TC01727H

[44] Martin Weigel, Tong Lu, Gilles Bailly, Antti Oulasvirta, Carmel Majidi, and Jürgen Steimle. 2015. iSkin: Flexible, Stretchable and Visually Customizable On-Body Touch Sensors for Mobile Computing. In *Proceedings of the 33rd Annual ACM Conference on Human Factors in Computing Systems (CHI '15)*. ACM, New York, NY, USA, 2991–3000. https://doi.org/10.1145/2702123.2702391

[45] Martin Weigel, Aditya Shekhar Nittala, Alex Olwal, and Jürgen Steimle. 2017. SkinMarks: Enabling Interactions on Body Landmarks Using Conformal Skin Electronics. In *Proceedings of the 2017 CHI Conference on Human Factors in Computing Systems (CHI '17)*. ACM, New York, NY, USA, 3095–3105. https://doi.org/10.1145/3025453.3025704

[46] Michael Wessely, Theophanis Tsandilas, and Wendy E. Mackay. 2016. Stretchis: Fabricating Highly Stretchable User Interfaces. In *Proceedings of the 29th Annual Symposium on User Interface Software and Technology (UIST '16)*. ACM, New York, NY, USA, 697–704. https://doi.org/10.1145/2984511.2984521

[47] Anusha Withana, Daniel Groeger, and Jürgen Steimle. 2018. Tacttoo: A Thin and Feel-Through Tattoo for On-Skin Tactile Output. In *Proceedings of the 31st Annual ACM Symposium on User Interface Software and Technology (UIST '18)*. ACM, New York, NY, USA, to appear.

[48] Junichi Yamaoka, Ryuma Niiyama, and Yasuaki Kakehi. 2017. BlowFab: Rapid Prototyping for Rigid and Reusable Objects Using Inflation of Laser-cut Surfaces. In *Proceedings of the 30th Annual ACM Symposium on User Interface Software and Technology (UIST '17)*. ACM, New York, NY, USA, 461–469. https://doi.org/10.1145/3126594.3126624

[49] Sang Ho Yoon, Ke Huo, Yunbo Zhang, Guiming Chen, Luis Paredes, Subramanian Chidambaram, and Karthik Ramani. 2017. iSoft: A Customizable Soft Sensor with Real-time Continuous Contact and Stretching Sensing. In *Proceedings of the 30th Annual ACM Symposium on User Interface Software and Technology (UIST '17)*. ACM, New York, NY, USA, 665–678. https://doi.org/10.1145/3126594.3126654

[50] Yang Zhang, Gierad Laput, and Chris Harrison. 2017. Electrick: Low-Cost Touch Sensing Using Electric Field Tomography. In *Proceedings of the 2017 CHI Conference on Human Factors in Computing Systems (CHI '17)*. ACM, New York, NY, USA, 1–14. https://doi.org/10.1145/3025453.3025842

[51] Ruike Zhao, Shaoting Lin, Hyunwoo Yuk, and Xuanhe Zhao. 2018. Kirigami enhances film adhesion. *Soft Matter* 14 (2018), 2515–2525. Issue 13. https://doi.org/10.1039/C7SM02338C